is too small to permit its resolution to within the experimental uncertainty (±10%), reliable measurements could not be obtained below 100 amp. The radiative contribution is normalized with respect to the total wall heat flux. These results are compared with measurements of Barzelay[5] (obtained for a similar arc configuration but with an entirely different radiation gage) and the theoretical results of Clark and Incropera.[6] Although the favorable comparison which exists between the three sets of results is, by itself, insufficient to completely certify the validity of the proposed technique, it does suggest that the method merits further consideration for use with plasma, as well as other high-temperature, gas flows.

It is recognized that the most critical aspect of the proposed diagnostic method is the assumption that insertion of the radiation gage in the duct does not appreciably alter the radiation field or the thermal state of the plasma. To determine whether such alterations had a significant bearing on the results, additional measurements were performed using a radiation gage with both surfaces reflecting. The results obtained for the total wall heat flux to each of the surfaces for the reflector vs reflector combination compared favorably with the heat flux values for the reflecting surface in the black vs reflector combination. Moreover, total wall heat flux measurements were made for the standard segments adjoining the radiation gage, first with the gage in place and then with the gage replaced by a standard segment, and no appreciable difference in the measurements was observed. Together, these results suggest that there is no significant alteration of the radiosity distribution or the thermal state of the plasma and that, at least for situations in which radiation is not the dominant contribution to the wall heat flux, the proposed technique may be used for reliable measurements.

References

[1] Lukens, L. A., "An Experimental Investigation of Electric Field Intensity and Wall Heat Transfer for the Heating Region of a Constricted Arc Plasma," Ph.D. thesis, 1971, Purdue Univ., Lafayette. Ind.

[2] Yakubov, I. T., "Energy Emitted by an Argon Plasma in Spectral Lines," *Optics and Spectroscopy*, Vol. 19, No. 4, 1965, pp. 277–281.

[3] Hermann, W., "Energy Transport by Radiation with Absorption in Cylindrical Arcs," *Zeitschrift für Physik*, Vol. 216, No. 1, Jan. 1969, pp. 33–44.

[4] Drummeter, R. and Hass, G., "Solar Absorptance and Thermal Emittance of Evaporated Coatings," *Physics of Thin Films*, edited by G. Hass, Vol. 2, Academic Press, New York, 1964, pp. 305–361.

[5] Barzelay, M. E., "Continuum Radiation from Partially Ionized Argon," *AIAA Journal*, Vol. 4, No. 5, May 1966, pp. 815–822.

[6] Clark, K. J. and Incropera, F. P., "Thermochemical Nonequilibrium in an Argon Constricted Arc Plasma," AIAA Paper 71-593, Palo Alto, Calif., 1971.

Effect of Transition on Three-Dimensional Shock-Wave/Boundary-Layer Interaction

ROBERT H. KORKEGI*

Aerospace Research Laboratories, Wright-Patterson Air Force Base, Ohio

Introduction

FOR two-dimensional shock-wave/boundary-layer interaction, shock impingement on a surface occurs at a constant spanwise Reynolds number whereby the boundary layer is either laminar, transitional, or turbulent. In the three-dimensional case, shock waves are generally skewed with respect to the flow direction on a surface so that the shock impingement line may cover a wide Reynolds number range. Thus, a single shock may interact with a boundary layer which is initially laminar, then transitional, and finally turbulent.

The purpose of this Note is to identify the effect of boundary-layer transition on three-dimensional shock interactions and thus provide the correct interpretation of some anomalous flow patterns.

Received October 20, 1971.

* Director, Hypersonic Research Laboratory. Associate Fellow AIAA.

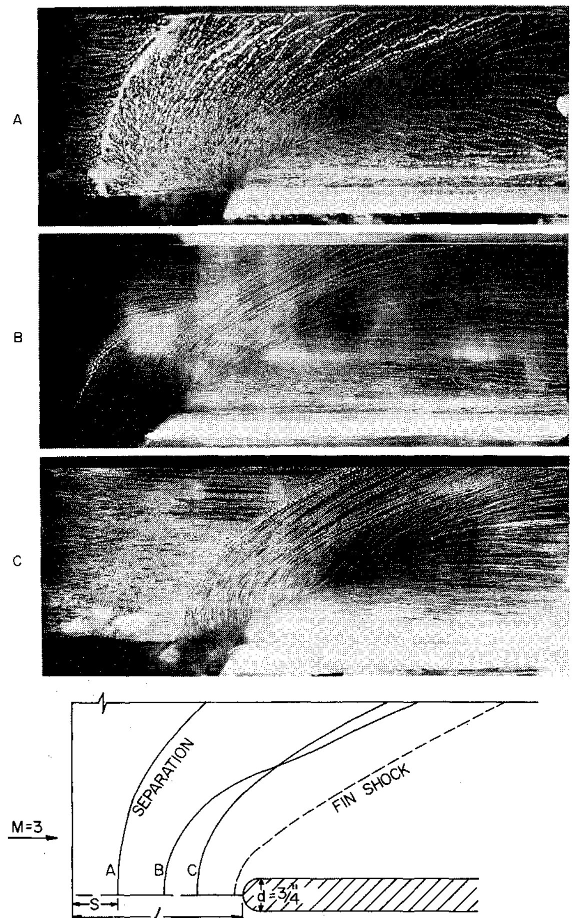

	l/d	$Re_l \times 10^{-6}$	$Re_s \times 10^{-6}$
A LAMINAR	5.67	0.14	0.06
B TRANSITIONAL	3	1.85	0.36
C TURBULENT	5.67	3.50	2.40

Fig. 1 Blunt fin-flat plate interaction $-d = \frac{3}{4}$ in. (oil flow photographs from the study of Ref. 2).

Shock Interaction due to Blunt Protuberances

The curved bow shock of a blunt protuberance on a body, interacting with the body boundary layer causes widespread separation of a highly three-dimensional nature. As is the case for two-dimensional flow, the extent of separation is considerably greater for laminar than for turbulent interaction.[1,2]

Figure 1 shows oil flow photographs from the study of Ref. 2 illustrating flow separation due to the impingement of the bow shock of a $\frac{3}{4}$-in.-diam blunt fin on a sharp flat plate of 9-in. span at a Mach number of 3 and over a wide range of Reynolds numbers. For the low Reynolds number case of Fig. 1A, the interaction is entirely laminar whereas for the high Reynolds number case of Fig. 1C, it is totally turbulent and the upstream and lateral extent of interaction is markedly smaller. For the intermediate Reynolds number case of Fig. 1B there is a clear break in the separation line at a Reynolds number of approximately $\frac{3}{4}\times 10^6$, beyond which it has an inflection and

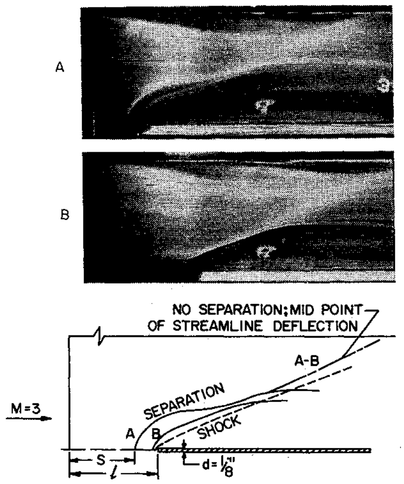

	l/d	$Re_l \times 10^{-6}$	$Re_s \times 10^{-6}$
A TRANSITIONAL	18	1.37	0.82
B TURBULENT	34	2.60	2.43

Fig. 2 Blunt fin-flat plate interaction $-d = \frac{1}{8}$ in. (oil flow photographs from the study of Ref. 2).

subsequently approaches the turbulent line as indicated by the tracings in the sketch in Fig. 1. The initial interaction occurs with a laminar boundary layer. The break is associated with the onset of boundary-layer transition with an attendant decrease in lateral spread of the interaction zone as the boundary layer approaches a fully turbulent state. Note that separation causes a strong disturbance to the flow, and therefore the onset of transition for this case is not necessarily representative of that for flow on an undisturbed flat plate.

Figure 2 illustrates another case of transitional (A) and fully turbulent (B) interaction for the same basic model as in Fig. 1 except for a much smaller fin diameter. Figure 2A again shows a break and inflection in the separation line indicative of transitional flow. An additional feature in Fig. 2 is that, somewhat beyond the transition region in Fig. 2A, and at approximately the same position relative to the fin leading edge in Fig. 2B, no further separation is observed. Beyond this point the

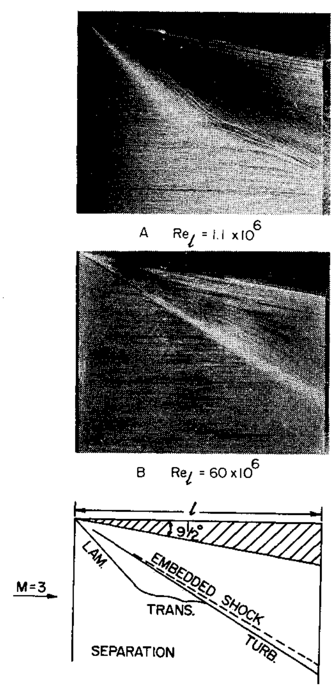

Fig. 3 Interaction in the corner of axially intersecting wedges (oil flow photographs from Ref. 3).

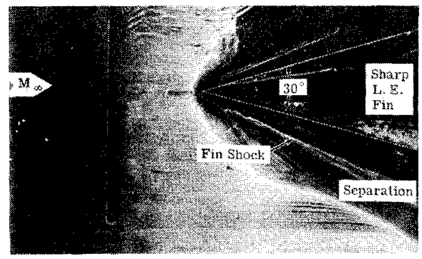

Fig. 4 Transitional interaction due to a sharp wedge on a flat plate at $M = 5$ (from Ref. 4).

decreasing strength of the fin bow shock is insufficient to cause separation of the turbulent boundary layer which remains attached with simply a deflection of the streamlines due to shock impingement. The inflection point of the streamlines is slightly upstream of the estimated two-dimensional bow shock shape as shown in the sketch in Fig. 2. This difference is probably due to distortion of the bow shock near the plate surface as a consequence of the upstream separated flow region. There is also a plate side-edge effect noticeable in the oil flow photographs, which could cause some distortion of the outboard flowfield, but should not affect the center region of interest.

As a final point, the horseshoe vortices generated by the upstream separated flow regions in Fig. 2A and B are seen to curve and proceed in a streamwise direction at the point beyond which no further separation occurs.

Shock Interaction due to an Axial Compression Corner

In a compression corner formed by the streamwise intersection of two wedges, embedded shocks, which may be viewed as a distorted continuation of the individual wedge bow shocks, impinge along the wedge surfaces causing lateral flow separation.[1] In the case of sharp-edged wedges with attached bow shocks, the inviscid flow field including the embedded shock impingement line is conical.

A recent study[3] over a wide Reynolds number range showed that the lateral extent of interaction due to shock impingement was considerably larger for laminar than for turbulent flow.

Figure 3A and B taken from Ref. 3 are oil flow photographs which show the interaction region in the corner of intersecting $9\frac{1}{2}°$ wedges at a Mach number of 3 for a low and a high Reynolds number, respectively.

Reference 3 points out that separation in Fig. 3A is initially due to laminar shock-wave/boundary-layer interaction, and the break in the separation line at a Reynolds number of approximately $\frac{1}{2} \times 10^6$ is caused by boundary-layer transition. Beyond transition, the interaction region and separation line eventually assume the pattern for fully developed turbulent flow. Figure 3B illustrates turbulent separation with a considerably narrower interaction region. In this figure, the laminar region is so small that it is virtually undetectable near the leading edge of the model. The sketch in Fig. 3 shows that turbulent separation in this case occurs just slightly upstream of the embedded shock wave.

Another example for a model akin to a corner is given in Fig. 4, taken from Ref. 4, which shows transitional separation due to interaction of the bow shock of a 30° wedge on a flat plate at a Mach number of 5.

Concluding Remarks

Other investigations of supersonic or hypersonic flow over three-dimensional configurations have exhibited similar distortions in separation lines; however, to the author's knowledge, the association of these distortions with boundary-layer transition has not heretofore been made.

In general, a three-dimensional shock wave-boundary layer interaction can be viewed locally as a two-dimensional one with cross flow and mass transfer[1]—a result of the scavenging vortex in the three-dimensional case. This interpretation is supported by experimental evidence which shows that the extent of a separated flow region is considerably greater for laminar than for turbulent flow for three-dimensional shock-wave/boundary-layer interaction as well as for the two-dimensional case. Thus, in retrospect, it is reasonable to expect a sharp change in the flow separation line as a skewed impinging shock crosses a region of boundary-layer transition. Conversely, a sharp change in an otherwise smoothly curved separation line on a planar surface is most likely indicative of transition because, in the absence of other disturbances in a flow, there is no physical mechanism whereby a shock generator of simple geometry should produce a distorted separation line.

References

[1] Korkegi, R. H., "Survey of Viscous Interactions Associated with High Mach Number Flight," *AIAA Journal*, Vol. 9, No. 5, May 1971, pp. 771–784.

[2] Young, F. L., Kaufman, L. G., II, Korkegi, R. H., "Experimental Investigation of Interactions between Blunt Fin Shock Waves and Adjacent Boundary Layers at Mach Numbers 3 and 5," ARL 68–0214, Dec. 1968, Aerospace Research Labs., Wright-Patterson Air Force Base, Ohio.

[3] West, J. E. and Korkegi, R. H., "Interaction in the Corner of Intersecting Wedges at a Mach Number of 3 and High Reynolds Numbers," ARL 71–0241, Oct. 1971, Aerospace Research Labs., Wright-Patterson Air Force Base, Ohio; also AIAA Paper 72–6, San Diego, Calif., 1972.

[4] Kaufman, L. G. II, Meckler, L., and Hartofilis, S. A., "An Investigation of Flow Separation on Aerodynamic Controls at Hypersonic Speeds," *Journal of Aircraft*, Vol. 3, No. 6, Nov.–Dec. 1966, pp. 555–561.

Technical Comments

Comment on "Lower Bounds on Deformations of Dynamically Loaded Rigid-Plastic Continua"

TOMASZ WIERZBICKI*

Institute for Fundamental Technical Research, Warsaw, Poland

Introduction

THE time and displacement bound technique in the early presentation (for example Ref. 1) was developed as a natural extension of the limit analysis theorems for rigid perfectly plastic bodies. While the upper bound principle was subsequently subjected to considerable refinement, no comparable progress was made in the lower bound theorems. A serious drawback in developing the theory further was the idea of kinematically admissible velocity field with stationary in time amplitude taken without alterations from static analysis. As a consequence lower bounds were obtained on the response time rather than on permanent displacements.

A remarkable contribution of Morales and Nevill,[2] is that, considering the amplitude of the velocity field as time variable, they indicated a way of finding lower bounds on displacements.

The objective of this Comment is to clarify some misinterpretations which appeared in Ref. 2 and to outline a correct proof of the new theorem. It should be noted that unlike the general inequality derived in Ref. 2, estimates obtained in all three illustrative examples are correct.

Separable Velocity Field

As a kinematically admissible velocity field $\dot{u}_i^*$, Morales and Nevill[2] took a one-degree-of-freedom velocity field

$$\dot{u}_i^*(x_i, t) = U_i^*(x_i)\dot{T}(t) \qquad (1)$$

where the mode function $U_i^*(x_i)$ satisfies kinematic boundary conditions while $\dot{T}(t)$ is a time-variable amplitude. For infinitesimal deformations the strain rate field $\dot{\varepsilon}_{ij}^*$ and dissipation function $D(\dot{\varepsilon}_{ij}^*)$ [resulting from Eq. (1)] are also of the separable form.

Received March 29, 1971; revision received June 25, 1971.

Index category: Structural Dynamic Analysis.

* Assistant Professor.

The first remark is that Eq. 1 should be substituted to both sides of the general inequality (8) of Ref. 2, yielding

$$\int_V D(E_{ij}^*)\,dV \int_0^{t_f} \dot{T}(t)\,dt \geqq \int_V (-\rho U_i^*)\left[\int_0^{t_f} \ddot{u}_i \dot{T}(t)\,dt\right] dV \qquad (2)$$

where $E_{ij}^* = \frac{1}{2}(U_{i,j}^* + U_{j,i}^*)$. Morales and Nevill introduced Eq. (1) only to one side of the aforementioned inequality and consequently were involved in unnecessary and lengthly computations.

Depending upon the choice of the function $\dot{T}(t)$ various information about the response of the body can be deduced. Assuming $\dot{T}(t) = V_o = \text{const}$, Martin[1] obtained from Eq. (2) a simple lower bound on the response time $t_f \leqq t_f^*$ where t_f^* is expressed in terms of U_i^* and initial velocity distribution $\dot{u}_i^o$. Recall that the response time is defined as such time at which actual velocities of all points $x_i \in V$ of the considered body vanish simultaneously

$$\dot{u}_i(x_i, t)\big|_{t=t_f} = 0, \quad u_i^f(x_i) = u_i(x_i, t)\big|_{t=t_f} = \int_0^{t_f} \dot{u}_i\,dt \qquad (3)$$

The corresponding value of the displacement is called permanent plastic displacement u_i^f.

The second remark is connected with the proper interpretation of these two definitions. To get lower bounds on permanent displacement a piece-wise linear function $\dot{T}(t)$ was assumed in Eq. (16) of Ref. 2. It is easy to verify, that when this function is substituted into Eq. (2), the lower bound theorem becomes

$$\delta \geqq \tfrac{1}{2} t_f^* \int_V \rho U_i^* \dot{u}_i^0\,dV \Big/ \int_V \rho U_i^* n_i\,dV$$

which now replaces Eq. (30) of Ref. 2.

Bounds on Vector and Scalar Quantities

The third remark relates to Ref. 2 and also to some previous work on that subject.[1] The application of impulsive loading theorems is straightforward in situatons when the displacement vector has only one component. However, the bounding theorems have been formulated for three-dimensional continua and in this case no satisfactory interpretation was given as to what quantity is in fact being bounded. Since formula (2) is of the energy type, one can expect to get from it bounds only on scalar quantities such as response time t_f or an absolute value of the displacement vector $\delta = \max \|u_i^f\|$, where $\|u_i^f\|$ denotes the natural norm of the vector u_i^f. In order to get bounds on δ it is therefore necessary to know a priori the direction cosines